AD-A041 142 GENERAL ELECTRIC CORPORATE RESEARCH AND DEVELOPMENT --ETC F/G 20/3
INVESTIGATION OF THE BEHAVIOR OF HIGH-ANISOTROPY PERMANENT MAGN--ETC(U)
MAY 77 J J BECKER N00014-74-C-0271
UNCLASSIFIED SRD-77-081 NL

| OF |
AD A041142

END

DATE FILMED
8-77

INVESTIGATION OF THE BEHAVIOR OF HIGH ANISOTROPY PERMANENT MAGNET MATERIALS

Final Report
to the
Office of Naval Research

Contract N00014-74-C-0271

Submitted by
J. J. Becker

May 1977

General Electric Company
Corporate Research and Development
Schenectady, NY 12301

SRD-77-081

UNCLASSIFIED

SECURITY CLASSIFICATION OF THIS PAGE *(When Data Entered)*

REPORT DOCUMENTATION PAGE	READ INSTRUCTIONS BEFORE COMPLETING FORM
1. REPORT NUMBER (9) Final Rept. 1 Mar 74-28 Feb 77.	2. GOVT ACCESSION NO. 3. RECIPIENT'S CATALOG NUMBER
4. TITLE (and Subtitle) (6) INVESTIGATION OF THE BEHAVIOR OF HIGH-ANISOTROPY PERMANENT MAGNET MATERIALS.	5. TYPE OF REPORT & PERIOD COVERED Final Report 74 Mar 01 - 77 Feb 28
	6. PERFORMING ORG. REPORT NUMBER (14) SRD-77-081
7. AUTHOR(s) (10) J. J. Becker	8. CONTRACT OR GRANT NUMBER(s) (15) N00014-74-C-0271
9. PERFORMING ORGANIZATION NAME AND ADDRESS General Electric Company Corporate Research and Development P. O. Box 8 Schenectady, NY 12301	10. PROGRAM ELEMENT, PROJECT, TASK AREA & WORK UNIT NUMBERS
11. CONTROLLING OFFICE NAME AND ADDRESS Office of Naval Research Electronics Program Office Arlington, VA 22217	12. REPORT DATE (11) May 77
	13. NUMBER OF PAGES
14. MONITORING AGENCY NAME & ADDRESS *(if different from Controlling Office)* (12) 33p.	15. SECURITY CLASS. *(of this report)* Unclassified
	15a. DECLASSIFICATION/DOWNGRADING SCHEDULE

16. DISTRIBUTION STATEMENT *(of this Report)*

Approved for public release; distribution unlimited.

17. DISTRIBUTION STATEMENT *(of the abstract entered in Block 20, If different from Report)*

18. SUPPLEMENTARY NOTES

19. KEY WORDS *(Continue on reverse side if necessary and identify by block number)*

20. ABSTRACT *(Continue on reverse side if necessary and identify by block number)*

This report describes investigations related to the origin of the magnetic coercive force in high-anisotropy materials that have taken place over a three-year period of contract support. Such materials with sufficiently high saturation magnetization supply the basis for the development of permanent magnets superior to anything currently available. A microsample technique developed in this work has made it possible to show for the first time that conventionally

(Continued on back)

DD FORM 1 JAN 73 1473 EDITION OF 1 NOV 65 IS OBSOLETE

UNCLASSIFIED

SECURITY CLASSIFICATION OF THIS PAGE *(When Data Entered)*

406677

1/B

(Continued)

sintered bulk Co_5Sm samples have magnetic properties that are defect-dominated in the same way as in particles, and show many magnetization phenomena previously seen only in single particles prepared from cast material. New measuring techniques were developed to make such observations possible. The potentially superior copper-modified alloys have been found to be dominated by domain wall pinning, in complete contrast to Co_5Sm, as shown by hysteresis loop analysis techniques that have been developed. Materials have been investigated in which both types of coercive force mechanisms coexist in the same sample and can be independently influenced. The distinction between nucleation and pinning domination is crucial to future alloy development as the desired structures are totally different.

ABSTRACT

This report describes investigations related to the origin of the magnetic coercive force in high-anisotropy materials that have taken place over a three-year period of contract support. Such materials with sufficiently high saturation magnetization supply the basis for the development of permanent magnets superior to anything currently available. A microsample technique developed in this work has made it possible to show for the first time that conventionally sintered bulk Co_5Sm samples have magnetic properties that are defect-dominated in the same way as in particles, and show many magnetization phenomena previously seen only in single particles prepared from cast material. New measuring techniques were developed to make such observations possible. The potentially superior copper-modified alloys have been found to be dominated by domain wall pinning, in complete contrast to Co_5Sm, as shown by hysteresis loop analysis techniques that have been developed. Materials have beer investigated in which both types of coercive force mechanisms coexist in the same sample and can be independently influenced. The distinction between nucleation and pinning domination is crucial to future alloy development as the desired structures are totally different.

TABLE OF CONTENTS

LIST OF ILLUSTRATIONS

Section 1

BRIEF SUMMARY

This is the final technical report for Contract N00014-74-C-0271, covering the period 1 March 1974 through 28 February 1977. The overall goal of this program has been to understand the origin of the coercive force in high-anisotropy materials so as to supply a basis for the development of permanent magnet materials surpassing the best available when this program began, which at that time were all based on Co_5Sm. The crucial requirement for such a material is a saturation magnetization greater than that of Co_5Sm, combined with high enough magnetocrystalline anisotropy to enable the development of a sufficiently high coercive force. The understanding of the factors that control this extremely structure-sensitive quantity has been the primary concern of this program.

Initially, other 5-1 and 17-2 compounds with easy-axis anisotropy were considered as suitable materials, closely analogous to Co_5Sm but potentially superior because of their higher M_S. There are two problems in all materials of this type. One is the origin of the properties of particles, and the other is the relationship between the properties of individual particles and those obtained in bulk magnets prepared by sintering. The microsample technique developed in this work has made it possible to show for the first time that bulk Co_5Sm magnets are defect-dominated in the same way as particles, showing many magnetization phenomena previously seen only in single particles prepared from cast material.

Obtaining the above results required detailed hysteresis loop measurements on samples often weighing less than a microgram. A novel and unconventional design was developed and incorporated in a new set of vibrating-sample-magnetometer pickup coils, permitting an order-of-magnitude improvement in signal-to-noise ratio.

At the work progressed, it became apparent that there is another class of materials with comparable potential, based on the copper-modified alloys of approximate composition $(Co, Cu)_7Sm$. These materials, in complete contrast to 5-1 and 17-2, owe their coercive force to domain wall pinning throughout the bulk of the material.

The analysis of the shapes of hysteresis loops, particularly as they depend on the value of the maximum magnetizing field H_m, has been developed into a powerful tool for the probing of magnetization reversal processes. This technique sharply makes the crucial distinction between nucleation-dominated and wall-pinning-dominated reversal.

It has been shown that the properties of the copper-modified alloys in optimum heat-treated condition are controlled entirely by wall pinning.

However, in other conditions of heat treatment it is possible to demonstrate both kinds of behavior in the same sample, to show that they depend differently on material constants, and even to vary them independently of each other.

Alloys of overall 7-1 composition are not in general single-phase. The prototype $(Co, Cu)_7Sm$ alloy appears to consist of a 5-1 and a 17-2 phase, each capable of a precipitation reaction producing a wall-pinning structure. However, in an alloy modified by a slight substitution of Fe for Co, both phases appear to have the 5-1 structure, in which a 17-2 precipitates. Studies of the type described above, together with measurements of anisotropy fields, have been made on these various component alloys and correlated with optical and electron microscopy to form a consistent picture of their metallurgical behavior as it determines their magnetic properties.

It is believed that the clarification of the distinction between nucleation and pinning, a theme that has appeared throughout this work, has contributed substantially to the understanding of the potential high-performance materials that have been identified, and thus to the goals of the work under this contract.

Section 2

INTRODUCTION

The extraordinary permanent magnet properties of Co_5Sm were discovered during an exploratory search at the General Electric Research and Development Center for materials combining high saturation magnetization (M_S) with high positive (easy-axis) magnetocrystalline anisotropy (K). Through the use of powder metallurgy techniques, Co_5Sm magnets are now fabricated with energy products greater than 20 million Gauss-Oersteds, several times higher than any material previously available.

Remarkable as it is, Co_5Sm represents a plateau in properties that can in principle be still further increased by a large amount. The key to such an increase is a higher M_S than Co_5Sm, along with a sufficiently high K to maintain a high enough coercive force H_C. One way of increasing M_S is to go to the 17-2 compounds, which have a structure closely related to that of the 5-1 materials. In some circumstances the 17-2 can have a K of the right sign, but in general these anisotropies have not been large enough to permit a sufficient H_C to take advantage of the larger M_S.

In both the 5-1 and 17-2 compounds, the coercive force is only a small fraction of the anisotropy field $2K/M_S$. This discrepancy, as well as many other aspects of the magnetic behavior of these materials, strongly suggested to us that magnetization reversal was not directly associated with the bulk properties of the material nor with classical fine-particle behavior, but was triggered at imperfections at which magnetic domain boundaries are formed or trapped. A great deal of work on single particles, summarized in about a dozen publications from this laboratory, has strongly reinforced this now generally accepted idea.

Through the use of microsample techniques reported below, it has been possible to show that the properties of sintered Co_5Sm magnets are also determined by magnetization reversal nucleation at defects, just as in single particles. Even when the density approaches 100%, the behavior is like that of isolated particles, a remarkable result.

There is an entirely different means of attaining high saturation magnetization with high coercive force, through the substitution of copper for some transition metal and the modification of the overall composition toward approximately 7-1. It is our present belief that the greatest promise for superior new materials is contained in some of these modified cobalt-rare-earths. Historically, copper additions were first made[1, 2] with the idea of replacing some of the cobalt in Co_5Sm with copper, giving compositions such as Co_3Cu_2Sm with the intent of producing small particles of Co_5Sm in a matrix of nonmagnetic Cu_5Sm. Castings of these materials had a remarkably high H_C, which could be

further increased by low-temperature heat treatments, but they suffered from low M_S because of the copper dilution. However, there have been a number of recent investigations[3, 4] of alloy series corresponding basically to $(Co,Cu)_xSm$ in which x varies from 5 to 8.5. These show a pronounced peak in properties at an x of about 7. Since typically only about 20% of the Co is replaced by Cu, these materials have a higher M_S than Co_5Sm. Their H_C, while not as high, is sufficient to permit the production of sintered magnets with energy products on the order of 20MGOe, which are now available from Shin-Etsu Ltd.

What makes this approach entirely different, from the point of view of structure control for magnetic properties, is that, in complete contrast to the 5-1 and 17-2 compounds, these materials owe their coercive force entirely to magnetic domain wall-pinning throughout the bulk of the material. Throughout this work, emphasis has been placed on the analysis of the shapes of hysteresis loops as a tool for the probing of magnetization reversal processes. This technique is particularly important in that it sharply distinguishes between nucleation-dominated and wall-pinning-dominated reversal. The distinction is vital to materials development, since the types of metallurgical structure desired are at opposite extremes for these two mechanisms. In nucleation-dominated material, defects are detrimental because they are the source of reversal nuclei. The ideal material would be homogeneous and defect-free. In wall-pinning-dominated material, effective pinning centers on the scale of perhaps tens or hundreds of angstrom units should be present everywhere in the material.

In this report Section 3 describes the microsample work, and Section 4 the vibrating-sample-magnetometer coils that made it possible. Section 5 discusses the reversal behavior of some copper-modified alloys, and Section 6 some aspects of the magnetic phase structure of 7-1 alloys.

Section 3

PROPERTIES OF MICROSAMPLES OF SINTERED COBALT - SAMARIUM MAGNETS*

ABSTRACT

Hysteresis loops of small but still multigrain samples taken from sintered Co_5Sm magnets show a wide range of behavior, samples from the same magnet bracketing the bulk properties. Magnetization discontinuities often appear and are associated with large grains. These jumps show a quantized dependence of jump field on magnetizing field and often a good $1/\cos\theta$ dependence, exactly as in particles prepared from cast material. A sample consisting of only one grain gave a completely rectangular loop. Measurements on sintered magnets indicate that large grains tend to reverse in small fields, detracting from the overall properties.

INTRODUCTION

It has become generally accepted that the magnetic reversal behavior of cobalt-rare-earth single particles is determined by defects through their influence on the nucleation of domain boundaries.[5, 6] Strong support for this interpretation has come from direct observation of magnetization discontinuities and their dependence on magnetizing field,[7] angle,[5] and other variables. It is much less clear how the behavior of sintered magnets should be interpreted -- whether they are like particles plus interactions, or whether some other model, involving perhaps grain-boundary phases[8] should be developed for them ab initio. This report describes experiments on small samples taken from sintered magnets in which exactly the same behavior can be observed as in particles prepared from cast material.

EXPERIMENTAL PROCEDURE AND RESULTS

Samples were prepared by breaking from bulk sintered magnets. Large particles thus obtained were further broken into samples of the desired size, usually on the order of 50 to 100 μm, under the microscope. Hysteresis loops were measured in a simple vibrating-sample magnetometer using a modification of the Mallinson coil configuration.[9] All hysteresis loops shown were traced twice, to illustrate the degree of reproducibility attained.

The first sample prepared in this way was relatively large, weighing about 10^{-4} g. Its reversal began with a magnetization discontinuity, as shown in Figure 1. As the magnetizing field was decreased, the jumps suddenly appeared at lower fields. The angular dependence of the jump fields was an

*Supported in part by the Office of Naval Research.

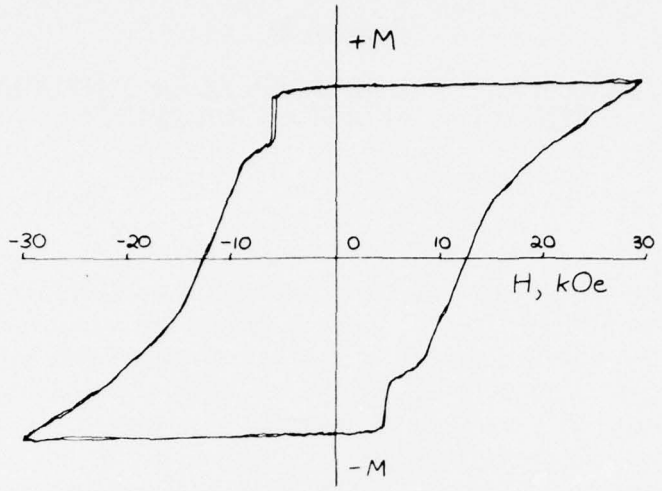

Figure 1. Hysteresis Loop of Microsample from Sintered Magnet

exact $1/\cos\theta$, but with angular offsets. Its behavior was very similar to that of a Co_5Gd particle reported on earlier.[5]

While there was nothing unusual in the appearance of this sample, the sintered magnet was observed to contain a number of grains that were conspicuously larger than the $\sim 10\mu$ average size. A sample was prepared so that one such grain comprised a substantial portion of it, the rest consisting of many small grains. Its hysteresis loop is shown in Figure 2. The narrow loop within the major loop is the result of cycling in ± 6 kOe just after the initial jump, showing the behavior of the free wall produced by the nucleating step. This behavior is exactly like that observed earlier in single particles of cast material.[10] It thus appears that the large grain is reversing completely once nucleated, followed by the higher-H_{ci} multigrain portion.

Measurement of a number of particles from the same magnet showed a considerable spread in properties, especially in magnets showing many relatively large grains. This spread bracketed the properties of the bulk magnet. For example, 11 samples from a magnet whose bulk H_{ci} was only 2.5 kOe showed a spread in H_{ci} from 1.5 to 9.4 kOe, with an average of 2.8. Thus, the particles removed by fracturing appear to represent a reasonable sample of the overall properties.

The influence of large grains was studied more closely by investigating two magnets, one made from powder as received from the jet mill, the other made from powder passed through a 400 mesh (38μ) sieve after jet milling. Fracture surfaces of the magnet made from unsieved powder showed occasional large grains, as in Figure 3(a). They were not observable in the other magnet, Figure 3(b). The hysteresis loops of small samples of the first magnet

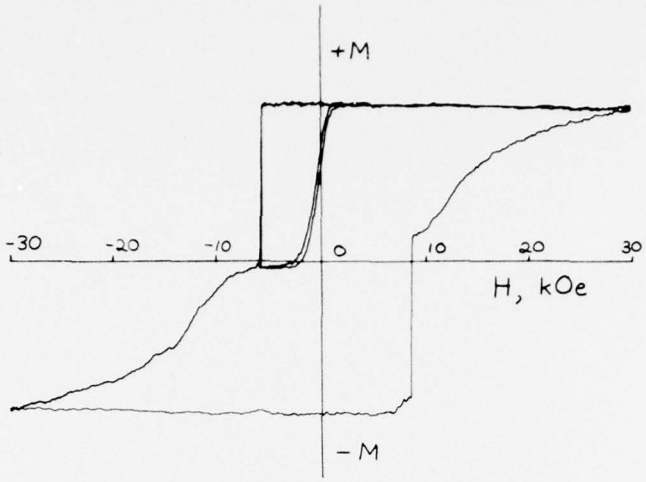

Figure 2. Hysteresis Loop of Sample Containing Large Grain and Smaller Grains

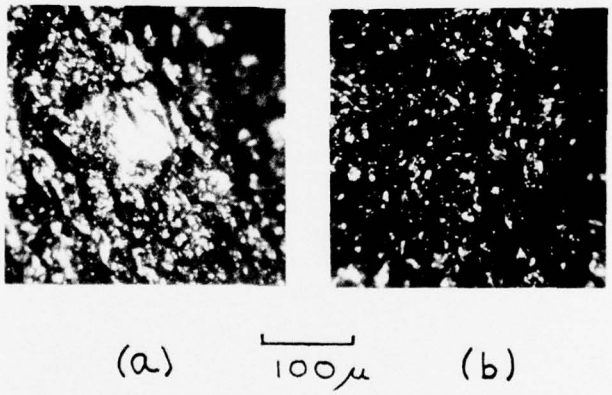

Figure 3. Fracture Surfaces of Magnets Sintered from (a) Unsieved and (b) Sieved Powders

characteristically showed a dropoff in magnetization early in the second quadrant, Figure 4(a). Samples from the second did not, Figure 4(b). In bulk properties, the second sample was somewhat superior to the first, having H_{ci} = 26.5 kOe and $(BH)_m$ = 22.2 MGOe, compared to 22.6 kOe and 19.8 MGOe. The complete loops for the small samples are drawn only to ±30 kOe magnetizing field and evidently are not completely saturated, as indicated by their asymmetry. Most loops showed this to some extent.

Then a sample consisting entirely of a thin portion of one large grain was excised from the first magnet. It is shown in Figure 5. It weighed approximately 5×10^{-7} g. Its hysteresis loop is shown in Figure 6. Again the complete reversal following nucleation is characteristic of individual grains. The

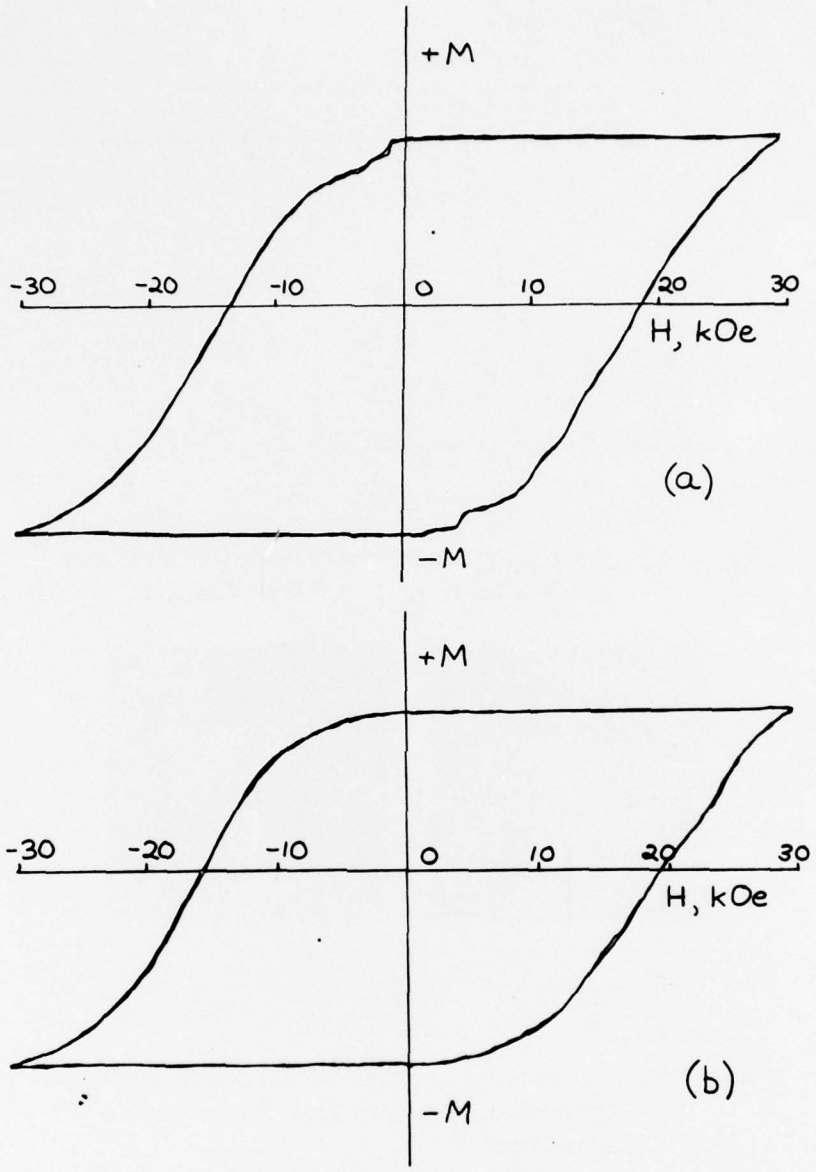

Figure 4. Hysteresis Loop of Microsample from Magnet Sintered from (a) Unsieved and (b) Sieved Powder

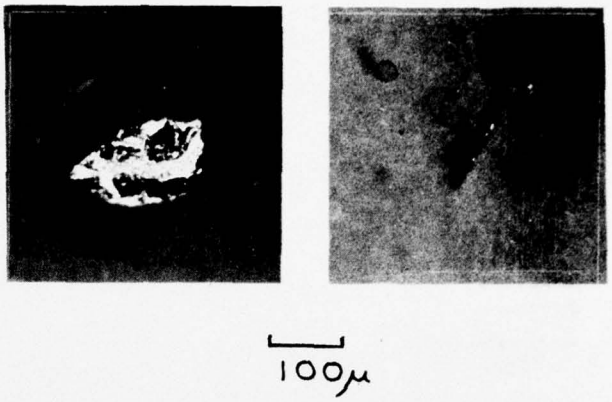

Figure 5. Microsample Consisting of Portion of Large Grain. Dark-field illumination.

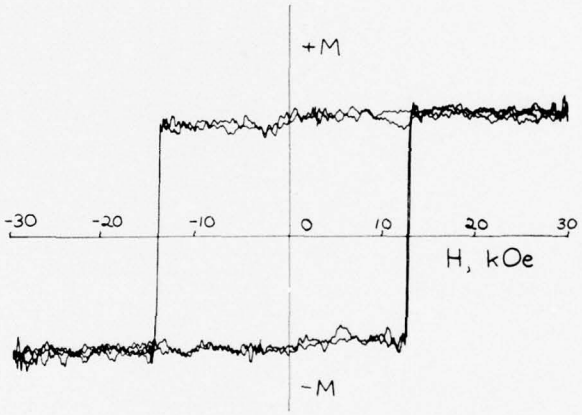

Figure 6. Hysteresis Loop of Sample Shown in Figure 5

fields at which this occurred are substantially below the bulk H_{ci}. However, they seem large considering that the surface of the particles as broken was not modified in any way. Large discontinuities and occasional rectangular loops were observed in other samples, sometimes in very low fields, sometimes not. Of course, the nucleation situation may be different when the grain is surrounded by its neighbors in bulk.

CONCLUSIONS

Measurements on tiny samples of sintered Co_5Sm magnets indicate a behavior entirely similar to that of single particles made from cast material. Large magnetization jumps are associated with large grains in the sintered material, consistent with the observation that sieving the starting powder appears to eliminate low-field magnetization dropoff in sintered magnets.

Section 4

SIMPLE VIBRATING - SAMPLE - MAGNETOMETER PICKUP COIL ARRANGEMENT*

ABSTRACT

A vibrating-sample-magnetometer pickup coil arrangement using only two coils whose axes are parallel to the applied field has the advantages of ease of balancing, adaptability to small gaps, freedom from image-effect problems, and good signal-to-noise performance.

SUMMARY

The purpose of this note is to describe a simple and effective vibrating-sample-magnetometer pickup coil arrangement that has been extremely useful in the measurement of microgram-sized samples of cobalt-rare-earth alloys in high fields.[11] The design incorporates the features discussed by Mallinson[12] but in a simple configuration of only two coils. It lends itself to use in a small gap. It also embodies the advantages of a small distance between coils and sample.[13] The arrangement is shown in Figure 7.

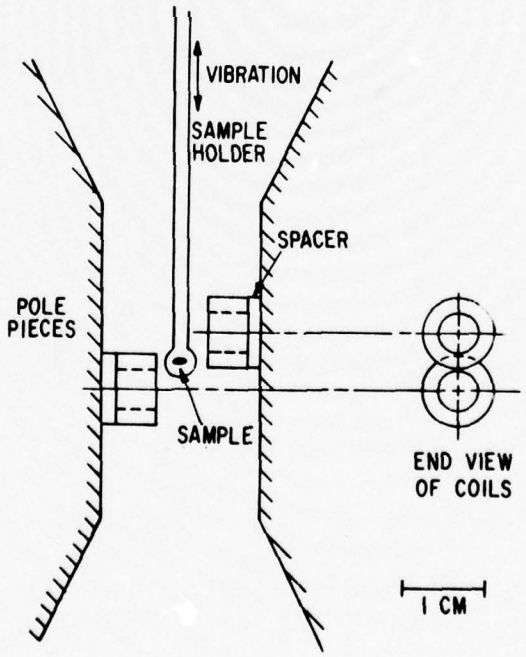

Figure 7. Vibrating-Sample-Magnetometer Coil Configuration

The coils are connected in series opposition. Exact balance is obtained by adjusting a high shunt resistance across the coil with the greater output as H

*Supported in part by the Office of Naval Research.

is varied without a sample. Somewhat surprisingly, this works much more satisfactorily than attempting to balance the conventional pair of vertical-axis coils. Even though the latter appear to have the advantage that their area-turns intercept no field, they are in practice much noisier, primarily because they are more sensitive to mechanical vibration. The small size and rigidity of the present coils make them quite easy to balance, and once adjusted they are very stable.

A second advantage is insensitivity to image effects. Vertical-axis coils proved troublesome in this respect, since their return windings respond to the time-varying field near the pole pieces, where the distortion of the dipole field by the image effect is greatest. In the present arrangement, almost all the signal comes from the coil windings nearest to the sample. In a rectangular-loop sample, any image effect would show up as a change in signal as H increases and the pole tips become saturated. Such changes caused difficulties with vertical-axis coils but, as can be seen in Figure 8 do not occur with the present arrangement.

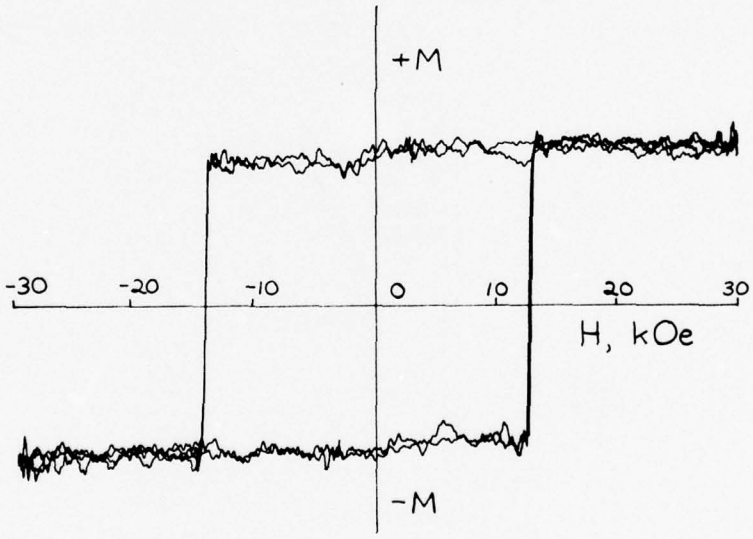

Figure 8. Hysteresis Loop of Single-Crystal Sample of Co_5Sm Weighing Approximately 5×10^{-7} g, in Maximum Field of 30 kOe (from Reference 11). $M_s \approx 5 \times 10^{-5}$ e. m. u.

Samples are usually mounted in paraffin inside the sealed-off narrow end of a disposable glass pipette, which has an outside diameter of about 1 mm. They are centered in the pronounced output saddle-point this arrangement provides. Figure 8 shows a hysteresis loop of a single-crystal sample of Co_5Sm weighing approximately 5×10^{-7} g, in a maximum field of 30 kOe, to indicate the signal-to-noise behavior that is routinely attainable.

Section 5

REVERSAL MECHANISM IN COPPER - MODIFIED COBALT - RARE - EARTHS*

ABSTRACT

The magnetization reversal in copper-containing cobalt-rare-earth permanent magnet materials can be completely dominated by pure bulk wall-pinning. This is shown by the form of hysteresis loops in varying magnetizing fields, whose appearance is in extreme contrast to those of unmodified cobalt-rare-earths, in which nucleation is the dominant factor in magnetization reversal. In some copper-modified materials it is possible to show both kinds of behavior in the same sample, with a sudden transition at a particular value of magnetizing field.

INTRODUCTION

Magnetization reversal in the cobalt-rare-earth permanent magnet materials is brought about by domain wall motion. The particles and grains are much larger than any relevant single-domain sizes,[14] the coercive forces are much too low for coherent rotation or curling, and the walls have been visually observed many times.

The coercive-force-determining process can be either the nucleation of walls which, once present, expand rapidly, or it can be bulk pinning of walls whose area does not change greatly. Structurally, nucleation is controlled by small numbers of relatively large defects while general pinning requires a distribution throughout the material of pinning agents such as precipitate particles whose dimensions are comparable to the wall thickness.

Cobalt-rare-earth particles, including Co_5Sm, show nucleation-dominated magnetization reversal. This has been established in many kinds of experiments, most directly by observation of magnetization discontinuities and their quantized dependence on magnetizing field,[15] their angular[16] and temperature[17] dependence, and their great sensitivity to surface treatment.[15] Particles from sintered magnets have also been shown to be nucleation-controlled.[18] In the closely related copper-modified cobalt-rare-earths, it is possible to observe equally pronounced pure wall-pinning behavior, as shown below. In spite of their basically similar composition and permanent magnet properties, their reversal takes place in a totally different way.

BEHAVIOR OF SUCCESSIVE HYSTERESIS LOOPS

The shapes of hysteresis loops as they depend on the value of magnetizing field H_m convey much information about the magnetization reversal process,

*Supported in part by the Office of Naval Research.

making a sharp distinction between nucleation-dominated and wall-pinning-dominated reversal. Two extreme kinds of behavior as a function of H_m can be envisioned. In a single particle of a material dominated by nucleation, walls whenever present move easily. In very low H_m this results in narrow loops sheared to the extent of the particle demagnetizing factor. In larger H_m a series of increasingly wider rectangular loops results, as in Figure 9a. The phenomenology of this behavior has been worked out in some detail.(19) For homogeneous bulk wall pinning, on the other hand, a plot of successive loops as a function of applied field looks like Figure 9b. Since the field necessary to move the wall is the same anywhere in the material, the coercive force is always the same, and only the remanence changes with H_m, within a range depending on the demagnetizing slope of the sample. For aggregates of particles, the considerable variations in individual nucleating fields would smooth out the rectangular behavior and give curves like Figure 10a for the nucleation case. For wall pinning, each particle is not dominated by a few defects but by the overall pinning structure, so an aggregate would not look much different from a single particle, as in Figure 10b. In the nucleation case, the remanence remains approximately the same while the loops shrink horizontally. In the pinning case, they stay the same width while shrinking vertically.

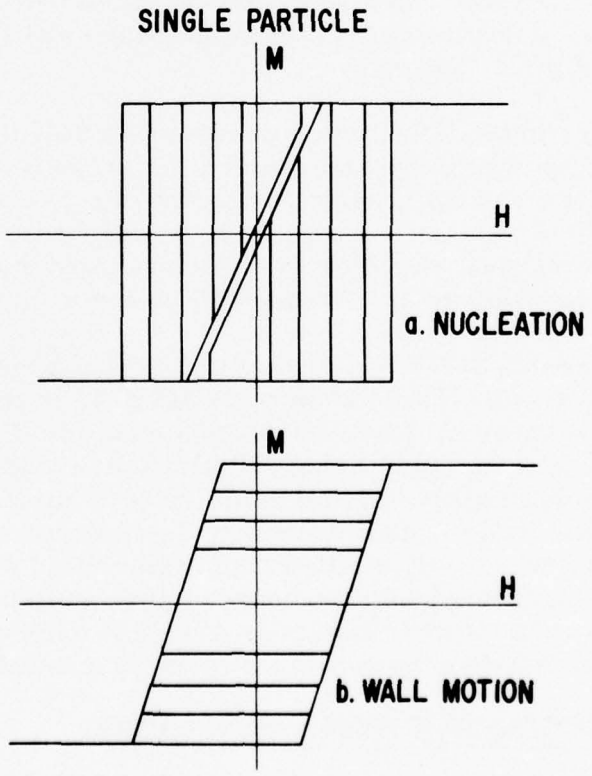

Figure 9. Hysteresis Loops Predicted for Single Particle as a Function of Magnetizing Field H_m; (a) Nucleation-Controlled Particle and (b) Pinning-Controlled Particle

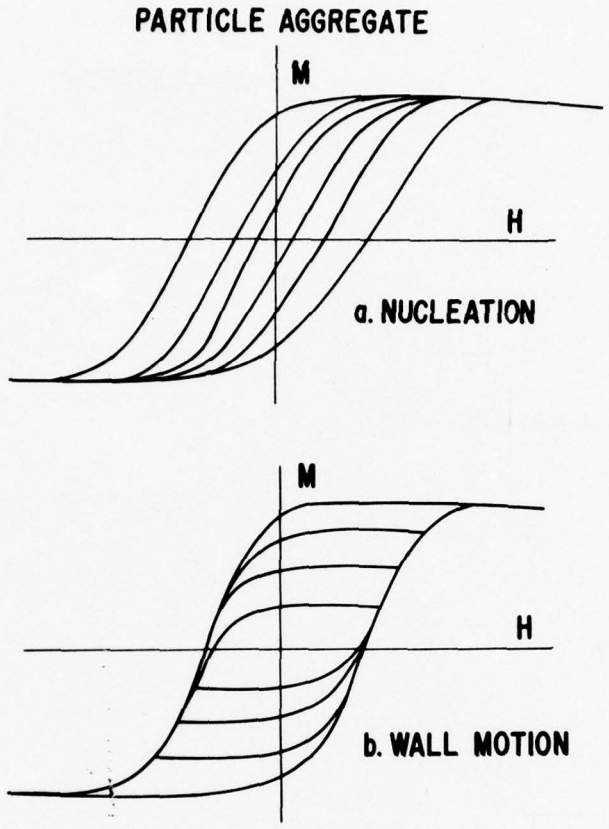

Figure 10. Hysteresis Loops Predicted for Aggregate of Particles as a Function of Magnetizing Field H_m; (a) Aggregate of Nucleation-Controlled Particles and (b) Aggregate of Pinning-Controlled Particles

RESULTS

Both extreme kinds of behavior can be strikingly illustrated by cobalt-rare-earth materials with and without copper modification. Figure 11a and 11b show series of hysteresis loops in varying H_m, for comparison with Figures 10a and 10b. Figure 11a is a 70 μm powder of Co_5Sm of relatively low coercive force. Figure 11b is a small piece of a sintered permanent magnet material obtained from Shin-Etsu Chemical Co., Tokyo, Japan.[20] Its composition is nominally $Sm(Co_{0.73}Cu_{0.14}Fe_{0.13})_7$ and it is based on developments by Tawara et al.[21] Its energy product is about 20 mGOe.

It is possible to observe both the extreme kinds of behavior illustrated above in the same material, and to influence them separately. Figure 12 shows the behavior of 70 μm particles of an as-cast alloy of composition

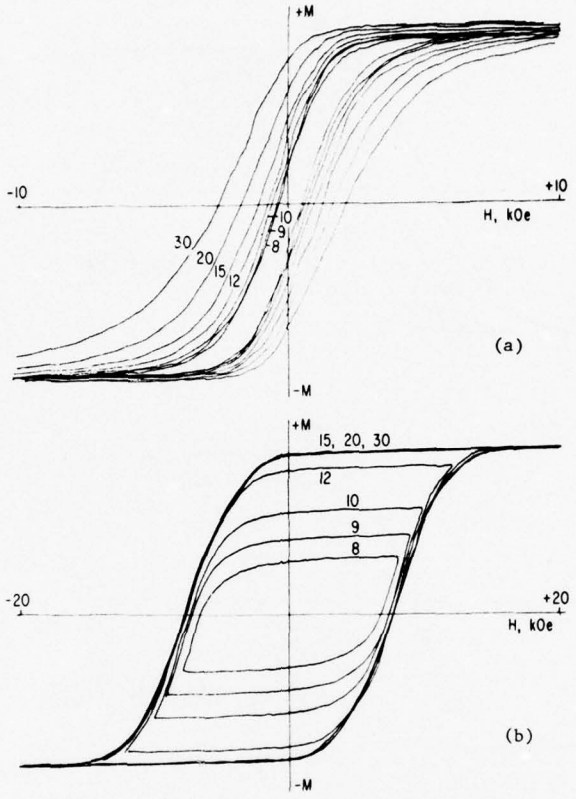

Figure 11. Observed Behavior of Aggregates of Particles; (a) Particles of Low-H_c Co_5Sm and (b) Particles of a Co-Fe-Cu-Sm Sintered Magnet

$Sm(Co_{0.81}Cu_{0.19})_{5.9}$. X-ray diffraction shows it to be essentially a single phase having the 1-5 structure. In fields above 8 kOe, the behavior is nucleation-dominated. In less that 8 kOe, the behavior suddenly switches to wall pinning with a constant H_c of about 1500 Oe. In nucleation-controlled particles, defects are often near the surface, with the result that the coercive force can be greatly influenced by surface treatment.[15] Some of the copper-modified particles were chemically polished for 30 seconds in a nitric-sulfuric-orthophosphoric-acetic acid mixture.[15] This resulted in the behavior shown in Figure 13. The coercive force in fields above 8 kOe was greatly increased, while the behavior in smaller fields was not changed. The polishing treatment removed surface nuclei and increased the nucleation-dominated coercive force. Once walls were present they still required about 1500 Oe to move, indicating pinning throughout the material just as before.

The Shin-Etsu material is known to consist of two kinds of grains with rather different domain structures[22] presumably because of a large-scale two-phase structure in the original cast material, resulting in grains of two different compositions. Similarly the $Sm(Co_{0.81}Cu_{0.19})_{5.9}$ is one of the two

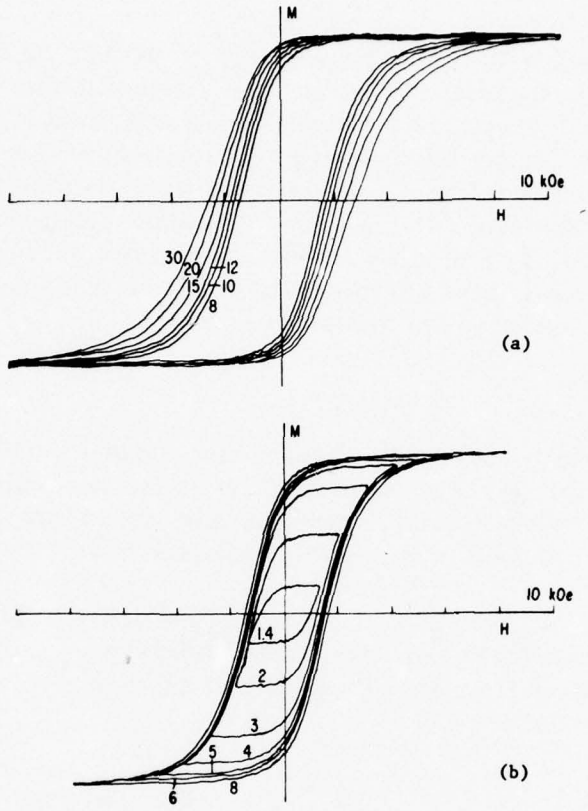

Figure 12. Hysteresis Loops in Varying H_m for ~70 μm Particles of a $Sm(Co_{0.81}Cu_{0.19})_{5.9}$ Alloy as Cast; (a) H_m = 8 kOe to 30 kOe and (b) Same Sample but H_m < 8 kOe. Numbers on curves are H_m in kOe.

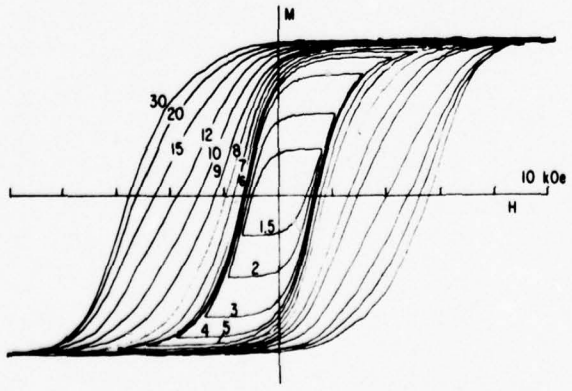

Figure 13. Hysteresis Loops in Varying H_m of Chemically Smoothed ~70 μm Particles of a $Sm(Co_{0.81}Cu_{0.19})_{5.9}$ Alloy as Cast. Numbers on curves are H_m in kOe.

compositions, along with $Sm(Co_{0.87}Cu_{0.13})_{7.5}$, occurring in castings of Sm $(Co_{0.84}Cu_{0.16})_{6.9}$, according to Menth.[23] Experiments on the $Sm(Co_{0.87}Cu_{0.13})_{7.5}$ composition showed a smaller wall coercive force of about 700 Oe and a similar very strong dependence of a large coercive force, up to about 3000 Oe, on surface treatment. In an alloy heat-treated for maximum permanent magnet properties, there must be submicroscopic precipitation providing pinning sites, presumably within each major composition. The fact that the heat-treated Shin-Etsu material consists of two separate compositions makes its ideal behavior even more remarkable.

CONCLUSIONS

The way in which successive hysteresis loops in varying maximum magnetizing fields differ is a strong indication of the reversal mechanism and is extremely distinctive for pure nucleation and pure pinning. Both kinds of behavior can be observed in the same material.

Unlike Co_5Sm magnets and their prototype materials, copper-modified magnets of approximately 1-7 composition show pure bulk wall-pinning behavior, in spite of the fact that they may consist of a mixture of grains of two different compositions.

Section 6

MAGNETIC PHASES IN COPPER - MODIFIED COBOLT - RARE - EARTH ALLOYS

The alloy of nominal composition $(Co_{0.8}Cu_{0.15}Fe_{0.05})_7Sm$, based on the work of Tawara and Senno, [24, 25] can be given very good permanent magnet properties. Several samples of this material were obtained, in peak aged condition, from M. Honshima of Shin-Etsu Chemical Industry Company, Takefu, Fukui, Japan. The processing steps reportedly used were: induction melting in argon, crushing in nitrogen, jet milling, pressing in a magnetic field of 10 kOe, isostatic pressing at 4 tons/cm^2, sintering for 1 hour at 1200 °C, quenching, and aging at 850 °C for 30 minutes. The as-received properties of these magnets were: saturation induction, 9.61 to 9.67 kG; remanence, 9.15 to 9.44 kG; intrinsic coercivity, 6.5 to 7.1 kOe; and maximum energy product, 19.9 to 21.2 MGOe.

This material contains grains of two different overall compositions, as indicated by optical microscopy, magnetic domain observations, and electron microprobe analysis. [26] According to Livingston[26] the great majority of the grains in this material have the composition $(Co_{0.79}Cu_{0.15}Fe_{0.06})_{7.5}Sm$. The others are $(Co_{0.74}Cu_{0.22}Fe_{0.05})_{6.4}Sm$. Presumably the two kinds of grains result from the grinding of an initially two-phase casting.

Another alloy of similar composition, $(Co_{0.84}Cu_{0.16})_{6.9}Sm$, has been reported to develop a remanence of 9200 G and a coercive force of 5000 Oe after 1 hour at 1230 °C followed by 1 hour at 790 °C. [27] This alloy as cast also consists of two large-scale phases, of compositions $(Co_{0.81}Cu_{0.16})_{5.9}Sm$ and $(Co_{0.87}Cu_{0.13})_{7.5}Sm$ (Ref. 27). We prepared all three of these compositions. X-ray diffraction indicated that as cast the 5.9 composition was mostly 5-1 phase, the 7.5 was mostly 17-2, and the 6.9 a mixture of both. It must be emphasized that here "5-1" and "17-2" refer to structures, not compositions. A 5-1 material can become rich in transition metal by replacing rare earth atoms by pairs of transition metal atoms. [28] As long as this is done randomly, the structure is 5-1. If it is done in an ordered way, the structure is 17-2, either hexagonal or rhombohedral depending on which of two types of ordering occurs. Figures 14, 15, and 16 show the domain structures of the cast alloys. The structure in Figure 16 is very similar to that of $Co_{17}Sm_2$. [29] The considerable corrugating of the walls is characteristic of a material of moderately high uniaxial anisotropy. Near the surface the walls develop the corrugated pattern in order to reduce the magnetostatic energy at the surface. If the anisotropy were extremely high, the wall energy would be too great to permit this and the walls would be relatively straight. This can be seen in occasional small areas of 1-5 phase in Figure 16. The same structure can also be seen in Figure 14, in which most of the material is 5-1. Figure 15 seems to have an intermediate structure, suggesting that it is two-phase on a rather fine scale under the casting conditions used.

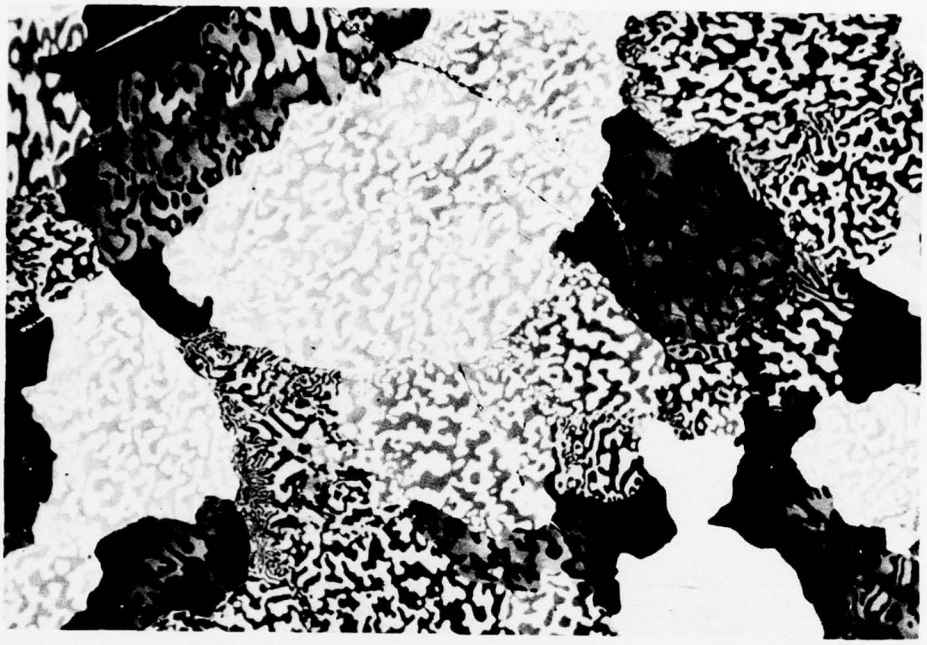

Figure 14. Magnetic Domain Structure of As-Cast $(Co_{0.81}Cu_{0.19})_{5.9}Sm$ Alloy (500x)

Figure 15. Magnetic Domain Structure of As-Cast $(Co_{0.84}Cu_{0.16})_{6.9}Sm$ Alloy (500x)

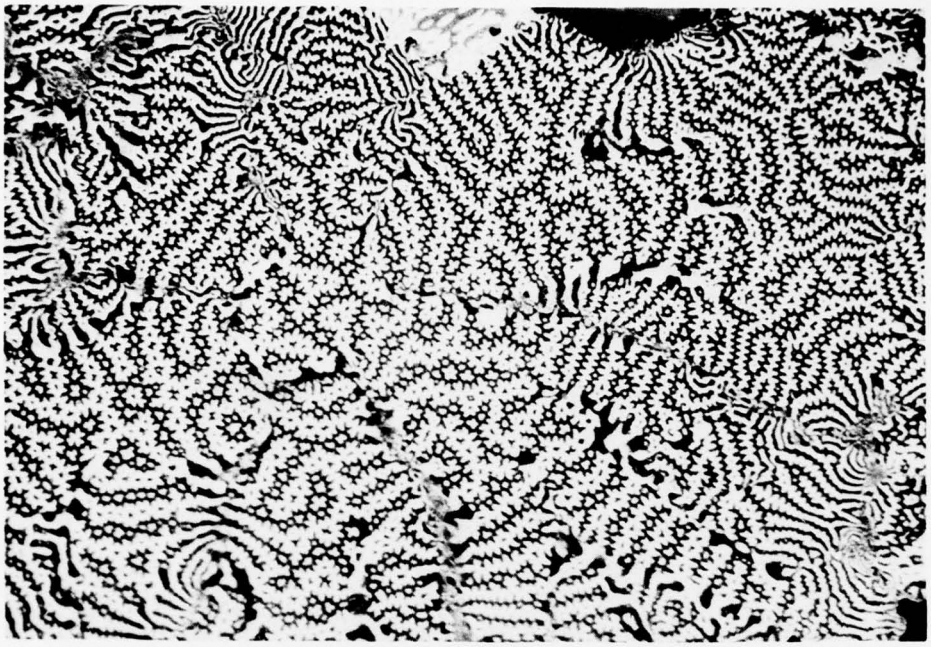

Figure 16. Magnetic Domain Structure of As-Cast $(Co_{0.87}Cu_{0.13})_{7.5}$ Sm Alloy (500x)

The anisotropy fields of these materials were also measured. This was done by measuring a sample of approximately 100 μm particles, aligned in a binder in a field, both parallel and perpendicular to the alignment direction and extrapolating as shown in Figure 17. The anisotropy fields are 460 kOe for the 5.9 material and 124 kOe for the 7.5 material. These are similar to the values generally obtained in Co_5Sm and $Co_{17}Sm_2$ respectively. The 6.9 material gives an intermediate value, 204 kOe.

It is remarkable that in both these alloys and the Shin-Etsu material, the best permanent magnet properties are developed in a material consisting of two major phases. These materials are completely dominated by wall pinning, as discussed in Section 5, so each major phase must have a very fine-scale precipitate as the wall pinning agent. In the Co-Cu-Sm alloys, presumably the 5-1 has a 17.2 precipitate and vice versa. In the Shin-Etsu material, although it would seem quite similar, the situation appears to be different.

Livingston and Martin[30] have studied the optimally aged Shin-Etsu material by transmission electron microscopy. They looked at the grains of 7.5 composition, which were in the majority. The structure they observed in the optimally aged condition is reproduced in Figure 18. The material consists of cells of one phase with a continuous boundary network of a second phase.

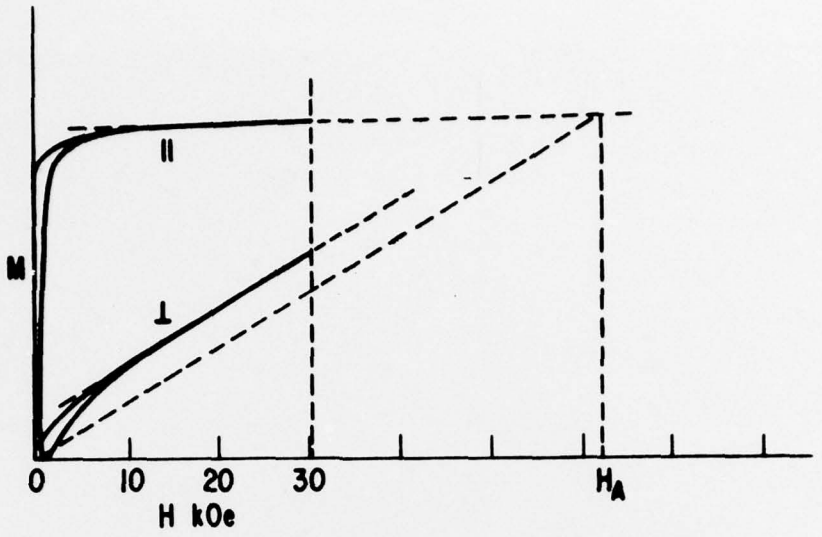

Figure 17. Measurement of Anisotropy Field H_A. Magnetization curves of aligned samples are drawn parallel and perpendicular to the alignment direction in a maximum field of 30 kOe and extrapolated as shown.

According to Livingston and Martin, analysis of electron diffraction patterns and dark-field micrographs indicates that the cell interiors have the 17-2 structure and the cell boundaries the 5-1 structure. The alloy was single-phase as quenched, and the cellular structure developed during annealing. In order for such a structure to be produced, the material must have been 5-1 on quenching, with the 17-2 cells developing during annealing until only the continuous network of 5-1 remains.

This interpretation seems very reasonable but one must comment that it implies the remarkable circumstance that both the 7.5 phase and the 6.5 phase must have the 5-1 structure. Then the phase separation occurring when the material is cast must be due to a miscibility gap, giving two equilibrium phases with the same structure but different compositions. As pointed out above, this is entirely possible, and in fact this behavior is shown by numerous metallurgical systems. However, it is a somewhat surprising variation on the behavior of cobalt-rare-earth alloys.

Anisotropy field measurements on these alloys do not really help to clarify the situation. The anisotropy field of the cast 6.5 alloy is 189 kOe, and that of the 7.5 alloy is 117 kOe. The Shin-Etsu material as quenched from 1200 °C has 141 kOe, and this quantity does not change much with various aging treatments. It is surprising that this alloy is not a closer analogue to the seemingly straightforward Co-Cu-Sm alloys.

(a)

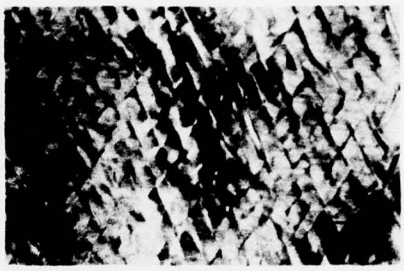

(b)

Figure 18. Cellular Microstructure of As-Received Co-Cu-Fe-Sm Magnet at Peak Aged Condition (aged 30 minutes at 850 °C): (a) Section Normal to Magnetic Alignment Direction (c-axis), (b) Section Including Alignment Direction (c-axis vertical). Cell interiors have the 17-2 structure, cell boundaries the 5-1 structure, with the phases fully coherent.

STABILITY OF PINNING-CONTROLLED MATERIAL

Whether a material is controlled by nucleation or by wall pinning has very different implications for its stability, especially in the form of small particles, such as might be used in a material consisting of permanent magnet particles imbedded in a matrix of some kind. Nucleation-controlled materials are very characteristically sensitive to surface treatment, as most of the reversal nuclei are created or removed at the surface. This can be seen in the very large increase in H_c resulting from the removal of nuclei by surface polishing, as for example in a comparison of Figures 17 and 18 of Section 5. On the other hand, such materials are also more vulnerable to degradation by any process that adds surface nuclei, particularly oxidation. The oxidation of a bit of samarium even at one locality on the surface produces a cobalt-rich region of low magnetocrystalline anisotropy, which even

though it may be small serves as an effective reversal nucleus for the entire particle. Figure 19 shows H_c as a function of H_m for the same sample shown in Figure 18 and again after a period of one year at room temperature. Local cobalt-rich regions are becoming more and more effective reversal nuclei as they develop. The same process can be seen on a more rapid scale in Figure 20. This shows the H_c dependence on H_m for a sample of particles of <70 m size as ground and after 10 minute heating in air at 150 °C and 200 °C. Even at these low temperatures nuclei are rapidly formed. In both cases, the H_m dependence in high fields is eliminated, as nuclei of the non-deactivating type described in Reference 19 are formed.

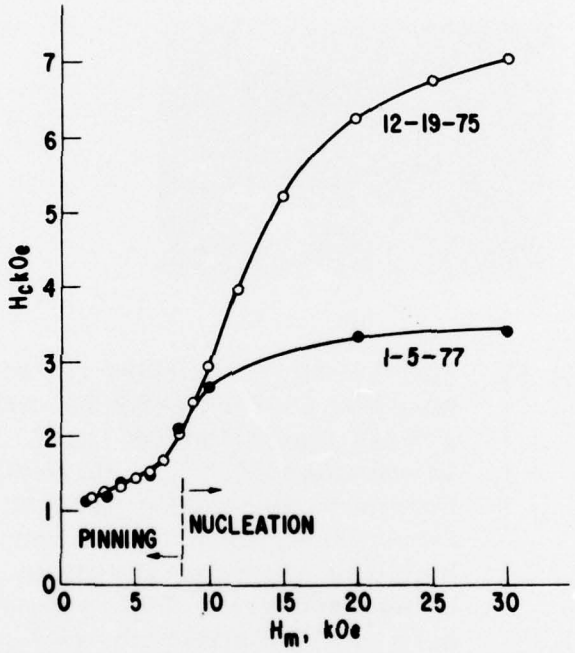

Figure 19. Coercive Force H_c as a Function of Magnetizing Field H_m for 70 μm Particles of $(Co_{0.81}Cu_{0.16})_{5.9}Sm$ Alloy. 12-19-75, after 30 seconds in 3 parts HNO_3 + 1 part HCl + 1 part H_3PO_4 + 5 parts CH_3COOH. 1-5-77, same sample after 12 1/2 months at room temperature.

In a sintered magnet of the Co_5Sm type, stability is attained by sintering to a density high enough to eliminate connected pores. If such a material is made into small particles it becomes increasingly susceptible to oxidation as the particle size is reduced and the surface-to-volume ratio increases. In the copper-modified materials, as can be seen in Figures 19 and 20, the wall-pinning component is not affected. If materials of this type have a sufficiently

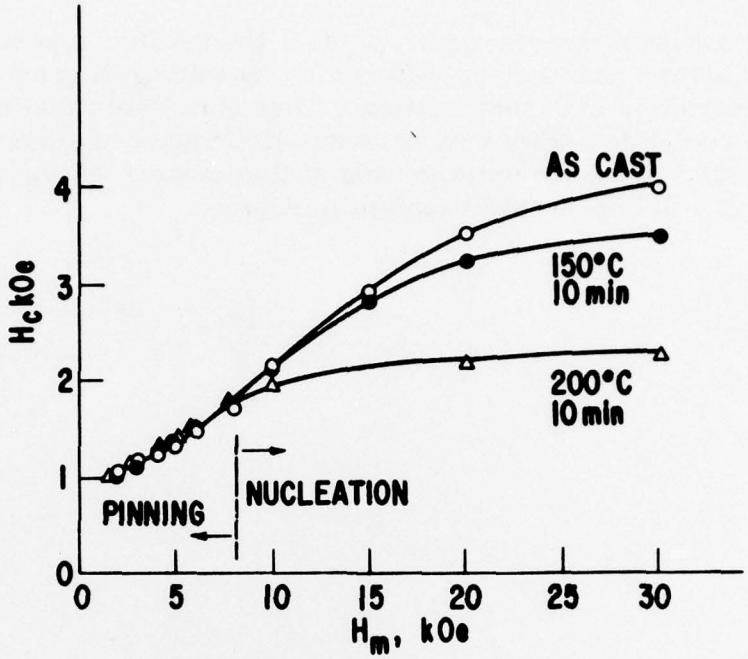

Figure 20. Coercive Force H_c as a Function of Magnetizing Field H_m for <50 μm Particles of $(Co_{0.81}Cu_{0.16})_{5.9}Sm$ Alloy, as Cast and After 10 Minutes in Air at 150 °C and 200 °C

high coercive force coming from wall pinning alone, they are not sensitive to surface condition or particle size and are inherently more suitable for applications in finely divided form.

COMPLEXITY OF PINNING - CONTROLLED MATERIAL

The different phase behavior of two alloys of similar overall composition prompts a general observation on this type of material. In a nucleation-controlled material, the coercive-force-limiting process is the provision of reversal nuclei at relatively large-scale imperfections. Composition enters only as it affects the overall anisotropy levels. On the other hand, coercive force control by generalized wall pinning requires a uniformly distributed submicroscopic precipitate structure of precisely the right size, shape, and magnetic characteristics. Such precipitates are generally produced by composition fluctuations within a given crystal lattice. The morphology of such structures is extremely sensitive to the energy of the surface between the precipitating phase and the matrix, and to its variation with the orientation of the surface. This energy in turn is extremely sensitive to composition, primarily as it affects lattice parameter and thus degree of misfit between precipitate and matrix. In the copper-modified cobalt-rare-earths, the

structure does not have cubic symmetry, so a change in composition may affect different lattice parameters differently, resulting in great changes in precipitate morphology with composition. Thus it is likely that a truly optimum pinning-controlled alloy may have small amounts of several elements present whose function is the optimization of this surface energy, just as with the small amounts of copper and titanium in Alnico.

Section 7

REFERENCES

1. E. A. Nesbitt, R. H. Williams, R. C. Sherwood, E. Buehler, and J. H. Wernick, Appl. Phys. Lett. 12, 361 (1968).
2. Y. Tawara and H. Senno, Japan. J. Appl. Phys. 7, 966 (1968).
3. Y. Tawara and H. Senno, Japan. J. Appl. Phys. 12, 761 (1973).
4. A. Menth, A. I. P. Conf. Proc. 29, 600 (1975).
5. J. J. Becker, A. I. P. Conf. Proc. 5, 1067-1071 (1972).
6. J. D. Livingston, A. I. P. Conf. Proc. 10, 643-657 (1973).
7. J. J. Becker, IEEE Trans. Mag. MAG-5, 211-214 (1969).
8. K. J. Strnat, A. I. P. Conf. Proc. 5, 1047-1066 (1972).
9. J. Mallinson, J. Appl. Phys. 37, 2514-2515 (1966).
10. J. J. Becker, *IEEE Trans. Mag.* MAG-7, 644-647 (1971).
11. J. J. Becker, A. I. P. Conf. Proc. 24, 676 (1975).
12. J. Mallinson, J. Appl. Phys. 37, 2514 (1966).
13. S. Foner, Ref. Sci. Instrum. 45, 1181 (1974).
14. J. D. Livingston, A. I. P. Conf. Proc. 10, 643-657 (1973).
15. J. J. Becker, IEEE Trans. MAG-5, 211-214 (1969).
16. J. J. Becker, A. I. P. Conf. Proc. 5, 1067-1071 (1972).
17. J. J. Becker, IEEE Trans. MAG-8, 520-522 (1972).
18. J. J. Becker, A. I. P. Conf. Proc. 24, 676-677 (1975).
19. J. J. Becker, IEEE Trans. MAG-9, 161-164 (1973).
20. I. T. Oiwa, M. Honshima, and E. Kikuchi, Proceedings of the 11th Conference on Rare Earth Research, 353-360 (1974).
21. Y. Tawara and H. Senno, Japan. J. Appl. Phys. 12, 761-762 (1973).
22. J. D. Livingston, J. Appl. Phys. 46, 5259-5262 (1975).

23. A. Menth. A. I. P. Conf. Proc. 29 (1976) (in press).

24. H. Senno and Y. Tawara, Japan. J. Appl. Phys. 47, 2671 (1975).

25. I. T. Oiwa, M. Honshima, and E. Kikuchi, Proc. 11th Rare Earth Research Conference, U. S. Atomic Energy Commission Technical Information Center, Oak Ridge, Tennessee, 353 (1974).

26. J. D. Livingston, J. Appl. Phys. 46, 5259 (1975).

27. H. Nagel, A. J. Perry, and A. Menth, J. Appl. Phys. 47, 2662 (1976).

28. K. H. J. Buschow and A. S. van der Goot, J. Less Common Metals 14, 323 (1968).

29. J. J. Becker, J. Appl. Phys. 41, 1055 (1970).

30. J. D. Livingston and D. L. Martin, J. Appl. Phys. 48, 1350 (1977).

DISTRIBUTION LIST FOR ONR ELECTRONIC AND SOLID STATE SCIENCES

	Copies
Director Advanced Research Projects Agency Attn: Technical Library 1400 Wilson Boulevard Arlington, Virginia 22209	1
Office of Naval Research Electronics Program Office (Code 427) 800 North Quincy Street Arlington, Virginia 22217	1
Office of Naval Research Code 105 800 North Quincy Street Arlington, Virginia 22217	6
Director Naval Research Laboratory 4555 Overlook Avenue, S. W. Washington, D. C. 20375	
Attn: Technical Library	6
Code 5200	1
5210	1
5270	1
6400	1
Office of the Director of Defense Research and Engineering Office of the Assistant Director Electronics and Physical Sciences The Pentagon, Room 3D1079 Washington, D. C. 20301	1
Defense Documentation Center Cameron Station Alexandria, Virginia 22314	12
Commanding Officer Office of Naval Research Branch Office 536 South Clark Street Chicago, Illinois 60605	1
San Francisco Area Office Office of Naval Research 50 Fell Street San Francisco, California 94102	1

	Copies
Commanding Officer Office of Naval Research Branch Office 1030 East Green Street Pasadena, California 91101	1
Commanding Officer Office of Naval Research Branch Office 495 Summer Street Boston, Massachusetts 02210	1
New York Area Office Office of Naval Research 715 Broadway - 5th Floor New York, New York 10003	1
ODDR&E Advisory Group on Electron Devices 201 Varick Street New York, New York 10014	1
Naval Air Development Center Attn: Technical Library Johnsville Warminster, Pennsylvania 18974	1
Naval Weapons Center China Lake, California 93555 Attn: Technical Library Code 6010	 1 1
Naval Research Laboratory Underwater Sound Reference Division Technical Library P.O. Box 8337 Orlando, Florida 32806	1
Navy Underwater Sound Laboratory Technical Library Fort Trumbull New London, Connecticut 06320	1
Commandant, Marine Corps Scientific Advisor (Code AX) Washington, D.C. 20380	1
Naval Ordnance Station Technical Library Indian Head, Maryland 20640	1

	Copies
Naval Postgraduate School Monterey, California 93940	
Attn: Technical Library	1
Electrical Engineering Department	1
Naval Missile Center Technical Library (Code 5632.2) Point Mugu, California 93010	1
Naval Electronics Laboratory Center San Diego, California	
Attn: Technical Library	1
Code 2300	1
2600	1
4800	1
Naval Undersea Center Technical Library San Diego, California 92132	1
Naval Weapons Laboratory Technical Library Dahlgren, Virginia 22448	1
Naval Ship Research and Development Center Central Library (Code L42 and L43) Washington, D.C. 20007	1
Naval Surface Weapons Center White Oak Laboratory Silver Spring, Maryland 20910	
Attn: Technical Library	1
Code 200	1
212	1
Deputy Chief of Naval Operations (Development) Technical Analysis and Advisory Group (Code NOP-077D) Washington, D.C. 20350	1
Commander Naval Air Systems Command Washington, D.C.	
Attn: Code 310	1
360	1
Commander Naval Electronics Systems Command Washington, D.C. 20360	
Attn: Code 304	1
310	1

	Copies
Commander Naval Sea Systems Command Washington, D. C. 20360	1
Naval Surface Weapons Center Attn: Library Dahlgren, Virginia 22448	1
Air Force Office of Scientific Research Attn: Electronic and Solid State Sciences Division Department of the Air Force Washington, D. C. 20333	1
Air Force Weapon Laboratory Technical Library Kirtland Air Force Base Albuquerque, New Mexico 87117	1
Air Force Avionics Laboratory Air Force Systems Command Technical Library Wright-Patterson Air Force Base Dayton, Ohio 45433	1
Air Force Cambridge Research Laboratory L. G. Hanscom Field Technical Library Cambridge, Massachusetts 02138	1
Harry Diamond Laboratories Technical Library Connecticut Avenue at Van Ness, N. W. Washington, D. C. 20438	1
U. S. Army Research Office Box CM, Duke Station Durham, North Carolina 27706	1
Director U. S. Army Engineering Research and Development Laboratories Fort Belvoir, Virginia 22060 Attn: Technical Documents Center	1
Director National Bureau of Standards Attn: Technical Library Washington, D. C. 20234	1

SUPPLEMENTAL LIST FOR ELECTROMAGNETICS

	Copies
Naval Research Laboratory 4555 Overlook Avenue, S. W. Washington, D. C. 20375	
Attn: Code 5300	1
7100	1
7900	1
Naval Electronics Laboratory Center San Diego, California 92152	
Attn: Code 2100	1
2200	1

SUPPLEMENTAL LIST FOR ELECTRONIC MATERIALS

Naval Research Laboratory 4555 Overlook Avenue, S. W. Washington, D. C. 20375	
Attn: Code 5220	1
5230	1
5250	1
5260	1
5270	1
5500	1
Naval Electronics Laboratory Center San Diego, California 92152	
Attn: Code 2500	1
4000	1

SUPPLEMENTAL LIST FOR SYSTEMS AREA

Office of Naval Research 800 N. Quincy Street Arlington, Virginia 22217 Attn: Code 430	2
Naval Research Laboratory 4555 Overlook Avenue, S. W. Washington, D. C. 20375 Attn: Code 5400	1

	Copies
Naval Electronics Laboratory Center San Diego, California 92152	
Attn: Code 3000	1
5000	1
5600	1
Air Force Office of Scientific Research Mathematical and Information Sciences Directorate 1400 Wilson Boulevard Washington, D. C. 20333	1